Temperature and Impurity Effects on Strongly Coupled Polaron in an Asymmetric Parabolic Potential Quantum Dot

H.-J. Li[a] and S.-P. Shan[b,*]

[a] *College of Physics and Intelligent Manufacturing Engineering, Chifeng University, China*
[b] *College of Physics and Electromechanics, Longyan University, China*

Received: 16.07.2024 & Accepted: 09.10.2024

Doi: 10.12693/APhysPolA.147.46 *e-mail: ssping04@126.com

Spin–orbit splitting of polaron in an asymmetric parabolic potential quantum dot under the influence of temperature and impurity is studied in the framework of variational technique and quantum statistical theory. The effective mass of the polaron is obtained by theoretical derivation. Due to the spin–orbit interaction, the effective mass of the polaron splits into two branches on the basis of zero spin-splitting effective mass. The dependence of effective mass spin-splitting of polaron on temperature is obtained. At the same time, the effects of electron–phonon coupling strength, polaron velocity, transverse and longitudinal confinement lengths, and Coulomb bound potential strength on polaron effective mass are also discussed by numerical calculation. The numerical results show that the effective mass is an increasing function of temperature, electron–phonon coupling strength, and Coulomb bound potential strength and is a decreasing function of velocity. The absolute value of spin-splitting effective mass is an increasing function of temperature, electron–phonon coupling strength, and Coulomb bound potential strength and is a decreasing function of velocity. An important conclusion is drawn that the effective mass of the heavy hole band is negative.

topics: asymmetric parabolic potential quantum dot, temperature, impurity, spin–orbit interaction

1. Introduction

The giant magnetoresistance effect was discovered by Fert and Gruenberg in 1988, which marked the birth of spintronics [1]. Using the charge and spin of electrons, information can be transmitted and stored, which can greatly improve the speed and efficiency of electronic devices. It is also possible to fabricate electronic devices with new physical properties by using the spin of electrons [2–4]. Up to now, the most famous spin device model is the transistor based on controlling electron spin proposed by Datta and Das in 1990 [5]. Since the publication of their article, many researchers around the world have conducted experimental and theoretical studies on the Rashba effect in low-dimensional quantum systems [6, 7]. For example, Babanli et al. [8] investigated the influence of Rashba spin–orbit interaction on the transport properties of the two-dimensional quantum ring with finite width in the presence of a uniform perpendicular magnetic field. The research results showed that the Rashba spin–orbit interaction destroyed the beating pattern. Zhao et al. [9] calculated the Rashba coefficient and Rashba spin splitting for the first subband of $Al_{0.6}Ga_{0.4}N/GaN/Al_{0.3}Ga_{0.7}N/Al_{0.6}Ga_{0.4}N$ quantum well (QW), each as a function of the thickness of the inserted $Al_{0.3}Ga_{0.7}N$ layer and the external electric field. Results show that the Rashba coefficient and the Rashba spin splitting in the $Al_{0.6}Ga_{0.4}N/GaN/Al_{0.3}Ga_{0.7}N/Al_{0.4}Ga_{0.4}N$ QW could be modulated by changing the relative thickness of GaN and $Al_{0.3}Ga_{0.7}N$ layers and the external electric field, thereby giving guidance for designing the spintronic devices. Using the variational method of Pekar, Li et al. [10] investigated the Rashba effect of polaron in a parabolic quantum dot. The condition for strong coupling between electric and longitudinal optical (LO) phonons in a parabolic quantum dot (QD) was studied in detail. At the same time, the relations of the bound polaron ground state energy with the parallel confinement length, the electron–LO phonon coupling constant, the perpendicular confinement length, and the Coulomb binding parameter were also studied by the same authors [11]. Electron spin has also been experimentally studied, e.g., by Qiu and Gui et al. [12], who studied the giant Rashba effect in HgTe quantum wells with inverted energy bands.

The spin–orbit splitting of III–V semiconductors is a linear term of momentum in the Hamiltonian of the system, which results in the dispersion relation of electron energy, and the energy is split from one parabola into two.

The Rashba effect was previously considered to be caused by the electric field at the interface of the heterojunction, but it has been proven that the influence of the electric field on the Rashba effect is small, and the main contribution comes from the asymmetry of the wave function at the interface [13]. In an asymmetric parabolic potential quantum dot, because the lattice structure is asymmetrical, there are special phenomena such as the spin–orbit coupling effect and rotational symmetry breaking of spin Hamiltonian. These phenomena give the asymmetric quantum dot a wide application prospect in spin transport and spin manipulation. It is easy to see that many studies have been conducted on the Rashba effect in the electronic system, and several people have done research on it in the field of polaron. The electron interacts with its surrounding phonon cloud to form a polaron. The lower the dimension, the stronger the electron–phonon coupling and the more significant the phonon effect. An asymmetric parabolic potential quantum dot has the property of zero dimension. Therefore, in recent years, many studies have been carried out on the properties of polaron in an asymmetric parabolic potential quantum dot using various theoretical methods. In this paper, the influence of temperature and impurity on the spin–orbit interaction of strongly coupled polaron in an asymmetric parabolic potential quantum dot is studied theoretically in the framework of variational technique and quantum statistical theory.

2. Theoretical model and derivation

We choose an asymmetric parabolic potential quantum dot structure in which the motion of an electron with heavy hole characteristics is strongly restricted in three dimensions. The electron is surrounded by hydrogenated impurities. We only consider the interaction between the electron and longitudinal optical phonon and ignore the interaction between the electron and interface optical phonon. The Hamiltonian of the system can be written as

$$H = \frac{\hat{p}^2}{2m} + \sum_k \hbar\omega_{LO}\, \hat{a}_k^+ \hat{a}_k + \frac{1}{2}m\omega_1^2\rho^2 + \frac{1}{2}m\omega_2^2 z^2 + \sum_k \left[V_k \hat{a}_k \exp(\mathrm{i}\boldsymbol{k}\cdot\boldsymbol{r}) + \text{h.c.}\right] - \frac{\beta}{r} + \mathrm{i}\,\frac{\alpha_R}{2\hbar^3}\left(\hat{p}_-^3\hat{\sigma}_+ - \hat{p}_+^3\hat{\sigma}_-\right). \tag{1}$$

In (1), the last term represents the spin–orbit interaction of the electron with heavy hole characteristics, where $\hat{p}_\pm = \hat{p}_x \pm \mathrm{i}\hat{p}_y$, $\hat{\sigma}_\pm = \hat{\sigma}_x \pm \mathrm{i}\hat{\sigma}_y$, and $\hat{a}_k^+$ ($\hat{a}_k$) is the creation (annihilation) operator of bulk longitudinal optical phonon with frequency ω_{LO} and wave vector $\boldsymbol{k}$. The electronic position vector is denoted as $\boldsymbol{r} = (\rho, z)$, and the transverse and longitudinal confinement strengths as ω_1 and ω_2, respectively. We set $l_1 = \sqrt{\frac{\hbar}{m\omega_1}}$ and $l_2 = \sqrt{\frac{\hbar}{m\omega_2}}$, where l_1 and l_2 are defined as the transverse and longitudinal confinement lengths, respectively.

Here, V_k is the Fourier component of electron–phonon interaction, and its expression is expressed as follows

$$V_k = \mathrm{i}\left(\frac{\hbar\omega_{LO}}{k}\right)\left(\frac{\hbar}{2m\,\omega_{LO}}\right)^{1/4}\left(\frac{4\pi\alpha}{V}\right)^{1/2}. \tag{2}$$

In the above equation, V stands for the volume of the crystal, and α is the electron–phonon coupling strength. The Coulomb bound potential energy is expanded as a series

$$-\frac{\beta}{r} = -\frac{4\pi\beta}{V}\sum_k \frac{1}{k^2}\exp\left(-\mathrm{i}\boldsymbol{k}\cdot\boldsymbol{r}\right). \tag{3}$$

Due to the strong coupling studied, we perform the second unitary transformation in (1). Under the adiabatic approximation, we take the unitary transformation operator as

$$\hat{U} = \exp\Big[\sum_k \left(\hat{a}_k^+ f_k - \hat{a}_k f_k^*\right)\Big]. \tag{4}$$

Here, f_k and f_k^* are variational parameter functions that can be obtained through variational techniques. Tokuta's improved linear combination operators are introduced in the following form

$$\hat{p}_j = \sqrt{\frac{m\hbar\lambda}{2}}\left(\hat{b}_j + \hat{b}_j^+ + P_{0j}\right), \tag{5}$$

$$\hat{r}_j = \mathrm{i}\sqrt{\frac{\hbar}{2m\lambda}}\left(\hat{b}_j - \hat{b}_j^+\right), \tag{6}$$

for $j = x, y, z$. Here, λ and P_0 are variational parameters, and λ represents the vibrational frequency of the polaron. The ground state trial wave function of the system is selected as

$$|\,\Psi_0\rangle = \left(c\,\chi_{1/2} + d\,\chi_{-1/2}\right)|0\rangle_a|0\rangle_b. \tag{7}$$

The vacuum state $|0\rangle_b$ of the $\hat{b}$ operator and the unperturbed zero phonon state $|0\rangle_a$ satisfy $\hat{b}_j\,|0\rangle_b = \hat{a}_k\,|0\rangle_a = 0$, while

$$\chi_{1/2} = \begin{pmatrix} 1 \\ 0 \end{pmatrix} \quad \text{and} \quad \chi_{-1/2} = \begin{pmatrix} 0 \\ 1 \end{pmatrix} \tag{8}$$

stands for spin-up and spin-down states, respectively.

The total momentum of the system is

$$\boldsymbol{P}_T = \boldsymbol{P} + \sum_k \hat{a}_k^+ \hat{a}_k\, \hbar\boldsymbol{k}. \tag{9}$$

In order to determine the effective mass of the polaron, we minimize the expected value of the quantity $\hat{U}^{-1}(H - \boldsymbol{u}\cdot\boldsymbol{P}_T)\hat{U}$ in the state $|\,\Psi_0\rangle$ by using $\boldsymbol{u}$, which is a Lagrange multiplier and will be in due course identified as the velocity of the polaron.

We have

$$F(\lambda, f_k, u, P_0) = \langle \psi_0 | \hat{U}^{-1}(H - \boldsymbol{u}\cdot \boldsymbol{P}_T)\hat{U}|\Psi_0\rangle, \tag{10}$$

so by minimizing F with respect to the variational parameters, we can determine parameters of f_k, λ, P_0 by using the variational method. Further, we obtain the expected value of momentum

$$P = \frac{1}{|u|}\left[\langle \Psi_0 | \hat{U}^{-1} H \hat{U} | \Psi_0\rangle - F\right] =$$

$$m\left[1 + \frac{2\alpha}{3\sqrt{\pi}}\left(\frac{\lambda}{\omega_{LO}}\right)^{2/3} \pm \left(\frac{m\alpha_R \lambda}{\hbar^2 u}\right)\right] u. \tag{11}$$

We can see from the above equation that u is the velocity of the polaron, and the effective mass of the strongly coupling polaron m^* is given by

$$m^* = m\left[1 + \frac{2\alpha}{3\sqrt{\pi}}\left(\frac{\lambda}{\omega_{LO}}\right)^{2/3} \pm \left(-\frac{m\alpha_R \lambda}{\hbar^2 u}\right)\right]. \tag{12}$$

From the above equation, it is found that the effective mass of the polaron experiences splitting under the influence of the Rashba spin–orbit interaction.

The mean number of phonons around the electron is

$$N = \langle \Psi_0 | \hat{U}^{-1} \sum_k \hat{a}_k^+ \hat{a}_k \hat{U} | \Psi_0\rangle = \frac{\alpha}{\sqrt{\pi}}\sqrt{\lambda}. \tag{13}$$

The properties of polaron are determined by the statistical mean of the electron–phonon system for various states. According to quantum statistics

$$\bar{N} = \left[\exp\left(\frac{\hbar\omega_{LO}}{k_B T}\right) - 1\right]^{-1}. \tag{14}$$

The value of λ in (12) is related to N, and the relationship between m^* and T can be obtained by combining equations (12)–(14).

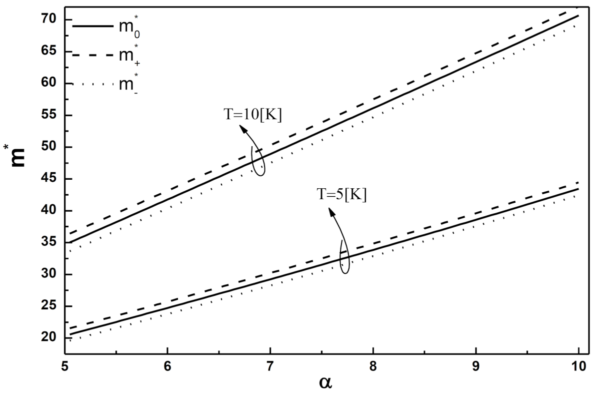

Fig. 1. The relationship between the effective mass m^* of polaron and the electron–phonon coupling strength α at different values of temperature T.

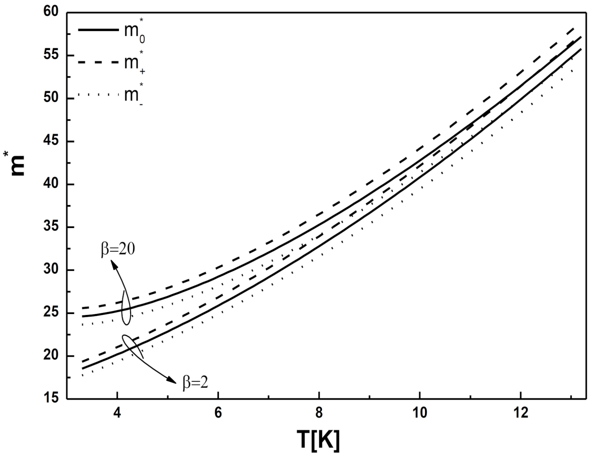

Fig. 2. The relationship between the effective mass m^* of polaron and the temperature T at different values of Coulomb bound potential strength β.

3. Numerical calculation and result discussion

To investigate the effects of temperature and impurity on Rashba spin–orbit interaction, we obtain the expression for the effective mass of strongly coupled bound polaron in an asymmetric parabolic potential quantum dot by theoretical derivation. The variation of polaron effective mass with temperature, Coulomb bound potential strength, transverse confinement length, longitudinal confinement length, electron–phonon coupling strength, and velocity are discussed separately. In order to simplify the calculation, polaron units $2m = 1$, $\hbar = 1$, and $\omega_{LO} = 1$ are used. The numerical results are shown in Figs. 1–8. In Figs. 1–5, the solid line represents the zero spin effective mass m_0^*, the dashed line represents the spin-up splitting effective mass m_+^*, and the dotted line shows the spin-down splitting effective mass m_-^*.

For fixed $u = 2$, $\alpha_R = 1$, $\beta = 10$, $l_1 = 0.6$, and $l_2 = 1$, Fig. 1 shows the relationship between the polaron effective mass m^* and the electron–phonon coupling strength α when the temperature T takes different values. One can see from this figure that the effective mass is an increasing function of the electron–phonon coupling strength. This is because when the electron–phonon coupling strength increases, the interaction between the electron and its surrounding phonons is enhanced, so the effective mass of the polaron increases. It can be also seen that the effective mass splits into two branches on the basis of zero spin-splitting effective mass. This is due to the Rashba spin–orbit splitting caused by the asymmetry structure of the asymmetric quantum dot. When the temperature is fixed, the change in the splitting gap is not significant with the increase of electron-phonon coupling strength. We find that the higher the temperature is, the greater the effective mass of the polaron is. Because high

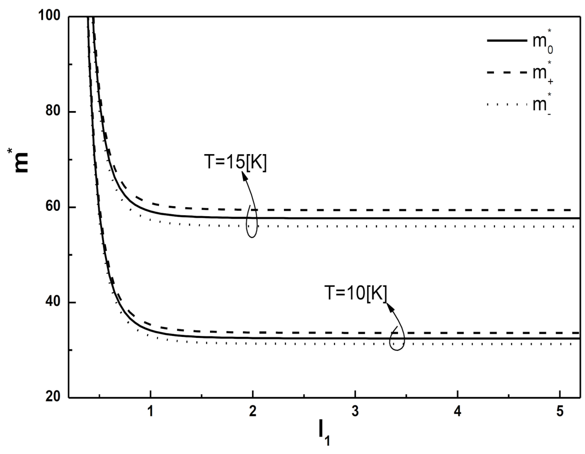

Fig. 3. The relational curve between the effective mass m^* and the transverse confinement length l_1 when the temperature T takes different values.

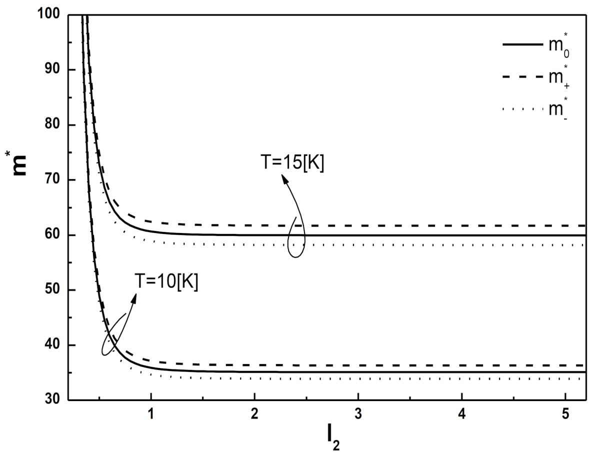

Fig. 4. The relational curve between the effective mass m^* and the longitudinal confinement length l_2 when the temperature T takes different values.

temperature increases the degree of crystal polarization, the number of longitudinal optical phonons increases with the increase in temperature. At the same time, a higher temperature will also accelerate the thermal motion of electron and phonons. For these reasons, the electron interacts with more phonons. Therefore, the increase in temperature will increase the polaron effective mass. In the figure, the effective mass splitting distance increases as the temperature increases. It is shown that temperature has a positive impact on the effective mass spin-splitting.

For the fixed values of $u = 2$, $\alpha_R = 1$, $\alpha = 6$, $l_1 = 0.6$, and $l_2 = 1$, Fig. 2 depicts the relationship between the effective mass m^* of the polaron and the temperature T with different values of the Coulomb bound potential strength β. As can be seen from this figure, the effective mass of the polaron splits into two curves based on zero spin-splitting effective mass and increases with the increase in temperature. The conclusion is the same as for Fig. 1. The change in the effective mass splitting-distance is not obvious with the increase in temperature and the Coulomb bound potential strength. We find that the effect of the Coulomb bound potential strength on the effective mass becomes smaller with the increase in temperature.

Given $u = 2$, $\alpha_R = 1$, $\alpha = 6$, $\beta = 10$, and $l_2 = 1$, the results presented in Fig. 3 show the relationship between the effective mass m^* of the polaron and the transverse effective confinement length l_1 with $T = 10$ K and $T = 15$ K. For the fixed values $u = 2$, $\alpha_R = 1$, $\alpha = 6$, $\beta = 10$, and $l_1 = 0.8$, the results in Fig. 4 depict the relationship between the effective mass m^* of the polaron and the longitudinal effective confinement length l_2 with $T = 10$ K and $T = 15$ K. It can be seen from Figs. 3 and 4 that the effective mass of the polaron is a decreasing function of the transverse and longitudinal effective confinement lengths. The motion of the electron is affected by the confinement potential, and the larger the confinement potential, the more local the motion of the electron is. The electron–phonon interaction is enhanced as the motion range of the particle decreases, which causes the electron to interact with more phonons around it. From the expressions for $l_1 = \sqrt{\frac{\hbar}{m\omega_1}}$ and $l_2 = \sqrt{\frac{\hbar}{m\omega_2}}$, we find that the effective confinement length is inversely proportional to the square root of the confinement potential. The increase in the effective confinement length will reduce the number of phonons interacting with the electron, which will lead to a decrease in the polaron effective mass. It is also found from Figs. 3 and 4 that effective mass spin-splitting of polaron is not obvious when the transverse and longitudinal effective confinement lengths take small values. However, with the increase in transverse and longitudinal effective confinement lengths, the effective mass splitting distance increases and finally tends to the saturation value. Comparing Figs. 3 and 4, we find that the longitudinal effective confinement length has a greater effect on the effective mass of polaron than the transverse effective confinement length. It is also found from these two figures that the higher the temperature is, the larger the splitting distance is. This shows that the impact of temperature on effective mass splitting is positive, and this conclusion is the same as in Fig. 1.

For the fixed values $\alpha = 6$, $l_1 = 0.8$, $l_2 = 1.2$, $\alpha_R = 1$, and $T = 5$ K, the results presented in Fig. 5 show the relationship curve between the effective mass m^* of the polaron and the velocity u at different values of Coulomb bound potential strength β. As shown in this figure, the spin-up splitting effective mass and spin-down splitting effective mass change inversely with the increase in velocity. The splitting distance decreases as the velocity increases. The effective mass of zero spin-splitting does not change with the velocity of polaron. From the expression of polaron effective mass,

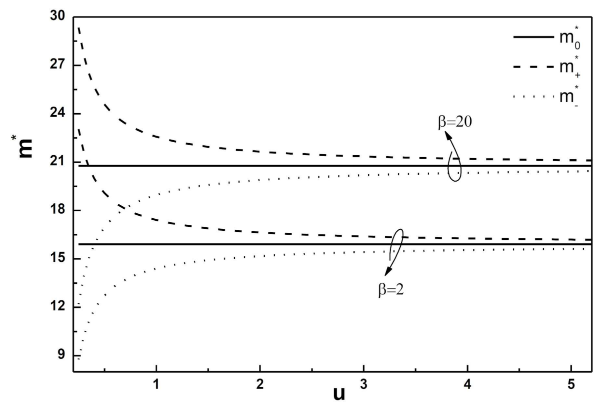

Fig. 5. The relationship between the effective mass m^* and the velocity u of polaron at different values of Coulomb bound potential β.

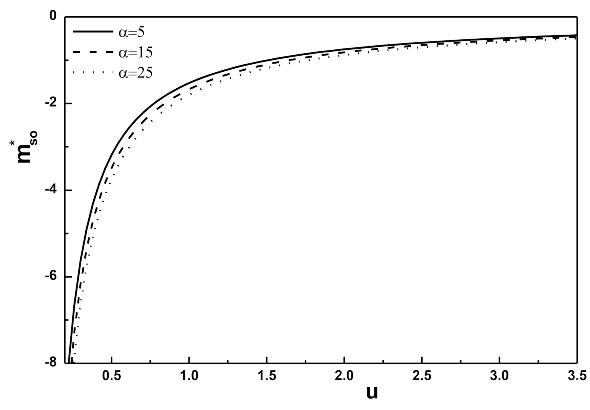

Fig. 7. The relationship between the effective mass of the spin–orbit split band m_{so}^* of polaron and the velocity u at different values of electron–phonon coupling strength α.

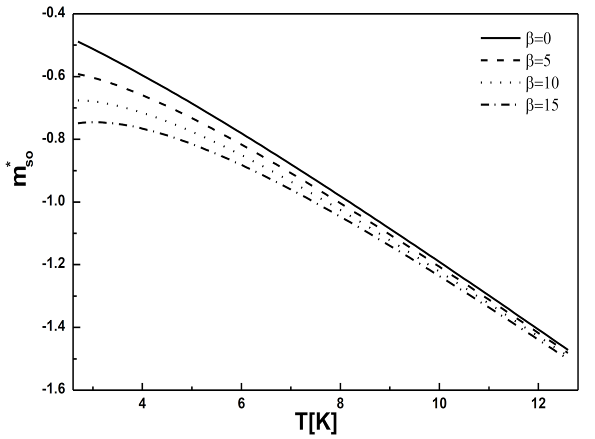

Fig. 6. The relational curve between the effective mass of the spin–orbit split band m_{so}^* and the temperature T at different values of Coulomb bound potential strength β.

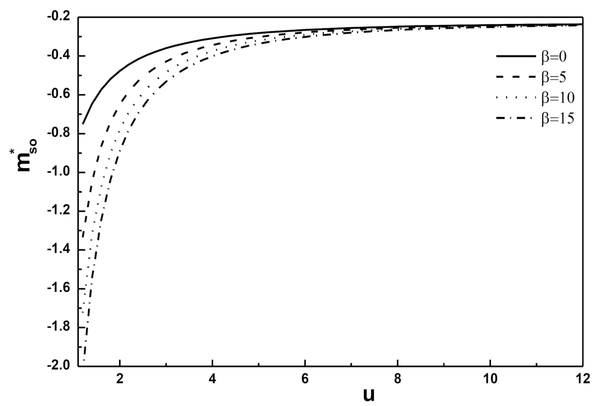

Fig. 8. The relationship between the effective mass of the spin–orbit split band m_{so}^* of polaron and the velocity u at different values of Coulomb bound potential strength β.

we find that the velocity is inversely proportional to the effective mass of the spin–orbit split band, which leads to the conclusion shown in Fig. 5. When the velocity is determined, the effective mass splitting distance does not increase significantly with the increase in the Coulomb bound potential strength. This conclusion is consistent with that in Fig. 2.

Given different values of Coulomb bound potential strength β, Fig. 6 depicts the change curve of the effective mass of the spin–orbit split band m_{SO}^* with the temperature T for fixed $\alpha_R = 0.5$, $\alpha = 6$, $l_1 = 0.8$, $l_2 = 1.2$, $u = 2$. One can see from this figure that the absolute value of spin-splitting effective mass is an increasing function of the temperature. When the temperature is taken as a certain value, the larger the Coulomb bound potential strength is, the larger the absolute value of the effective mass of the spin–orbit split band. It is also found from Fig. 6 that when the temperature $T < 4$ K, the Coulomb bound potential strength has a significant effect on the effective mass of the spin–orbit split band as the temperature changes. Outside this range, with the increase in temperature, the Coulomb bound potential strength has little effect on the effective mass of the spin–orbit split band, which is consistent with the conclusion in Fig. 2.

For the electron–phonon coupling strength taking different values, Fig. 7 describes the relationship between the effective mass of the spin–orbit split band m_{SO}^* and the velocity u for fixed $\alpha_R = 0.5$, $l_1 = 0.8$, $l_2 = 1.2$, $\beta = 5$, $T = 5$ K. It is found that when the velocity is fixed, the absolute value of the effective mass of the spin–orbit split band increases with the increase in electron–phonon coupling strength. When the velocity $u < 0.75$, the influence of electron–phonon coupling strength on the effective mass of the spin–orbit split band gradually increases with the increase in the velocity. When $u > 0.75$, the influence of electron–phonon coupling strength on the effective mass of the spin–orbit split band gradually decreases with the increase in the velocity. Given $\alpha_R = 0.5$, $l_1 = 0.8$, $l_2 = 1.2$, $\alpha = 6$, $T = 5$ K, Fig. 8 draws the relational curve between the spin-splitting effective mass m^*_{so} and the velocity u at different Coulomb bound potential strength β. When $u < 3$, the absolute value of the effective mass of the spin–orbit split band increases sharply with the decrease in the velocity. Outside this range, the spin-splitting effective mass changes slowly with the change in velocity. When $u < 5$, the Coulomb bound potential strength has a great influence on the effective mass of the spin–orbit split band.

An important phenomenon is found in Figs. 6–8, where the effective mass of the spin–orbit split band is negative, which is caused by the heavy hole characteristic of spin–orbit splitting. According to (14), it can be assumed that in Figs. 1–5, the effective mass spin-up splitting is flipped with the spin-down splitting.

4. Conclusions

Using Tokuda's improved linear combination operator method, we investigate the influence of temperature and impurity on the effective mass of strongly coupled polaron in an asymmetric potential parabolic quantum dot. Due to the asymmetric structure, the effective mass of polaron experiences Rashba spin–orbit splitting. The absolute value of the effective mass of the spin–orbit split band increases with the increase in temperature and the Coulomb bound potential strength. The effective mass of polaron is an increasing function of temperature, electron–phonon coupling strength, and Coulomb bound potential strength and is a decreasing function of velocity. In the study, we only consider the splitting of the heavy hole band, so the effective mass of the spin–orbit split band is negative.

Acknowledgments

This work was supported by the Scientific Research Project of Institutions of Higher Learning in Inner Mongolia Autonomous Region (Grant No. NJZY22137).

References

[1] F. Chi, L. Liu, *Int. J. Theor. Phys.* **57**, 562 (2018).

[2] L. Hong, J. Ge, S. Shuang et al., *Acta Physica Sinica* **39**(05), 728 (2022).

[3] E.I. Rashba, Al.L. Efros, *Phys. Rev. Lett.* **91**, 126405 (2003).

[4] S.-P. Shan, S.-H. Chen, *Iranian Journal of Science* **41**, 755 (2017).

[5] S. Datta, B. Das, *Appl. Phys. Lett.* **56**, 665 (1990).

[6] A. Hofmann, V.F. Maisi, T. Krähenmann, *Phys. Rev. Lett.* **119**, 176807 (2017).

[7] C.X. Zhang, A. Pfeuffer-Jeschke, K. Ortner et al., *Phys. Rev B* **65**(4), 5324 (2002).

[8] A.M. Babanli, O. Uçar, *Low Temp.Phys.* **47**, 849 (2021).

[9] Z.-Y. Zhao, H.-L. Wang, M. Li, *Acta Physica Sinica* **65**, 097101 (2016).

[10] W.P. Li, J.W. Yin, Y.F. Yu, J.L. Xiao, *J. Low Temp. Phys.* **160**, 195 (2010).

[11] J.W. Yin, W.P. Li, Y.F. Yu, J.L. Xiao, *J. Low Temp. Phys.* **163**, 53 (2011).

[12] Z.-J. Qiu, Y.-S. Gui, X.-Z. Shu, N. Dai et al., *Acta Physica Sinica* **53**, 1186 (2004).

[13] S.-P. Shan, *Low Temp. Phys.* **50**, 181 (2024).